

1 Image Analysis of Unusual Structures 2 on the Far Side of the Moon in the 3 Crater Paracelsus C

4
5 Mark J. Carlotto¹, Francis L. Ridge² and, Ananda L. Sirisena³
6 The Lunascan Project and Society For Planetary SETI Research
7
8

9 ABSTRACT

10
11 The authors present an analysis of Apollo 15 and Lunar Reconnaissance Orbiter images of two
12 unusual features in the crater Paracelsus C on the far side of the moon. At first glance these
13 structures appear to be walls or towers on the lunar surface. By combining multiple images we
14 show the larger feature, oriented in a northeast/southwest direction, is not simply a wall but
15 two walls on either side of a narrow valley or “passageway”. Using single image shape from
16 shading and 3D terrain visualization we show in a computer generated perspective view looking
17 northeast that the southwest end appears to be the entrance to the passageway. A reverse
18 angle view looking southwest shows the passageway ending at a rise of terrain at the other end,
19 possibly leading underground. The terrain surrounding the two structures is not flat but appears
20 “excavated” by some unknown mechanism, natural or artificial. It is shown that these objects
21 are visually different from the lunar background because their underlying structure is different.

22 1. Introduction

23 The search for extra-terrestrial intelligence (SETI) began in the 1960s with radio-telescopes
24 (Drake 1960) and has, to date, produced no positive evidence of its existence. During these early
25 years of SETI, Sagan (1963) spoke about the possibility of extraterrestrial visitation
26

27 “It is not out of the question that artifacts of these visits still exist, or even that some kind of
28 base is maintained (possibly automatically) within the solar system to provide continuity for
29 successive expeditions. Because of weathering and the possibility of detection and interference
30 by the inhabitants of the Earth, it would be preferable not to erect such a base on the Earth’s
31 surface. The Moon seems one reasonable alternative. Forthcoming high resolution photographic
32 reconnaissance of the Moon from space vehicles – particularly of the back side – might bear
33 these possibilities in mind.”
34

34

¹ mark@carlotto.us

² skyking42@gmx.com

³ anandals@aol.com

1 Foster (1972) estimated frequencies of visitations by extraterrestrials or their messenger probes
2 and suggested the possibility that past encounters may have left behind artifacts or indirect
3 evidence (e.g., deranged planetary terrain). Seeking a broader alternative to radio SETI, a search
4 for extraterrestrial artifacts (SETA) was proposed in the 1980s (Freitas 1983). The search for
5 alien artifacts on the moon (Arkhipov 1998, Davies and Wagner, 2013) is an outgrowth of this
6 more inclusive search strategy.

7
8 Davies (2012) called for a citizen science approach to SETI stating “rather than leaving SETI to a
9 small and heroic band of radio astronomers, we should mobilize the entire scientific community
10 to ‘keep their eyes open’ for telltale signs of alien technological activity.” One suggestion is to
11 look for evidence of mining or quarrying activities. Where on Earth the evidence may be buried
12 beneath overlaying strata, Davies believes “Quarrying or construction on the moon or asteroids
13 would persist conspicuously for much longer, and scrutiny of the Lunar Reconnaissance Orbiter
14 data would be a useful exercise.”

15
16 This paper provides evidence supporting the hypothesis that certain features in the crater
17 Paracelsus C on the far side of the moon may be artificial in origin. Section 2 summarizes the
18 discovery of these features – a case study in citizen science. Many times objects that appear
19 unusual in older lower resolution photographs turn out to be unremarkable in higher resolution
20 digital images. Analysis of LRO images in Section 3 including coregistered and “fused” images at
21 different sun angles reveals this is not the case. The question of artificiality in the context of the
22 surrounding terrain is considered in Section 4. Section 5 presents 3-D visualizations of the
23 features and the surrounding area to assist in their interpretation. Areas for future work are
24 discussed in Section 6.

25 2. Background

26 Reports of artificial structures on the moon in Apollo and Lunar Orbiter photographs are not
27 uncommon in the popular press and the Internet. Among the first were George Leonard’s 1976
28 book *Somebody Else is On the Moon* and Fred Steckling’s 1981 book *We Discovered Alien Bases*
29 *on the Moon* that identified a large number of unusual features in Lunar Orbiter and Apollo
30 photographs. Literally hundreds of reports can be found online today, many of which can be
31 traced back to these books.

32
33 Independent scientific groups such as The Lunascan Project⁴ and Society of Planetary SETI
34 Research⁵ investigate reported anomalies on the moon, Mars, and elsewhere. In May 2016,
35 SPSR member Ananda Sirisena notified Lunascan project coordinator Francis Ridge that he had
36 found an article posted on the Internet in 2014 reporting the discovery of unusual features on
37 the surface of the moon in the crater Paracelsus resembling dark “walls” or “towers”
38 photographed by the Apollo 15 astronauts⁶.

39
40 Ridge determined the coordinates of the features and located a high resolution Lunar
41 Reconnaissance Orbiter (LRO) image M118769870L that contained two unusual structures (Fig.

41

⁴ <http://www.astrosurf.com/lunascan/>

⁵ <http://spsr.utsi.edu>

⁶ <http://www.ufosightingsdaily.com/2014/01/new-moon-discovery-of-two-tall.html>

1 1). After finding the Apollo 15 panoramic camera image A15-P-8868 referenced in the article,
 2 Ridge realized the structures in the LRO image were the same features mentioned in the article.
 3 Sirisena then identified another Apollo 15 image (AS15-P-8873) over the same area taken at a
 4 different viewing angle. Three images acquired by two satellites from different viewing angles
 5 proved the features were not an optical illusion. Many times objects that appear unusual in
 6 older lower resolution photographs turn out to be unremarkable in higher resolution digital
 7 images. This was clearly not the case in the high resolution LRO image Ridge has found. The
 8 features appeared even more unusual up close. Three additional LRO M-frames were found
 9 using the Planetary Imagery Processing Environment (Fig. 2). In total, four LRO M-frames, two
 10 Apollo 15 P-frames, and five Apollo metric camera M-frames were located over the area (Table
 11 1).

12 3. Preliminary Image Analysis

13 Fig. 3a and Fig. 3b are map-projected images of the features of interest in M118769870L and
 14 M1168450258L, respectively. North is up. The larger feature (A) is oriented in a
 15 northeast/southwest direction. The smaller features (B) to the south is oriented in a
 16 northwest/southeast direction. In Table 1 the sun is to the west-northwest, illuminating the
 17 northwest side of feature A in frames M118769870L and M1115441699L. In M1153132512R and
 18 M1168450258L the sun is east-northeast, illuminating the southeast side of A. At this sun angle
 19 the terrain to the north casts a shadow along the northwest side.

20
 21 Using LRO image M118769870L and associated metadata⁷, the length of A is:

$$22 \quad L = M \times R = 235 \text{ pixels} \times 0.55 \text{ meters/pixel} = 129 \text{ meters} \quad (1)$$

23
 24 where M is its measured length in pixels and R is the pixel resolution. The length of B is 77
 25 meters.
 26

27
 28 The height of A can be calculated from the measured length of its shadow, N . Assuming for the
 29 moment the shadow is cast on flat terrain, the height at the northeast end is

$$30 \quad H = \frac{N \times R}{\tan \phi_i} = \frac{132 \text{ pixels} \times 0.55 \text{ meters/pixel}}{\tan 68.9^\circ} = 28.65 \text{ meters} \quad (2)$$

31
 32 where ϕ_i is the solar incidence angle. The height at the southwest end is about 19 meters. The
 33 height of the northeast end of A estimated from M1168450258L⁸ is 31.1 meters, which within
 34 10% of the first estimate (Eq. 2). Interestingly the height of B is slightly higher, about 29.5
 35 meters as estimated from M118769870L.
 36

37
 38 Combining multiple images reveal new information about these structures that is not evident in
 39 the original data. In Fig. 3c the two images have been merged by replacing shadowed pixels in
 40 one image with non-shadowed pixels in the other image, and vice versa. In Fig. 3a the sun is to

40

⁷ http://wms.lroc.asu.edu/lroc/view_lroc/LRO-L-LROC-3-CDR-V1.0/M118769870LC

⁸ http://wms.lroc.asu.edu/lroc/view_lroc/LRO-L-LROC-3-CDR-V1.0/M1168450258LC

1 the left, in Fig. 3b the sun is to the right. The resultant merged image reveals A is not simply a
 2 “wall” but appears to be two “walls” on either side of a narrow valley or “passageway” (Fig. 4a).
 3 B appears to have a ridge-like depression in the middle similar to A as shown in Fig. 4b. These
 4 details are discussed further in Section 5.

5 4. Lunar Context

6 These features are in the southwest corner of a 24 km crater named Paracelsus C. Paracelsus C
 7 is one of number of “satellite” craters of Paracelsus, an impact crater on the far side of the
 8 moon (Fig. 5). It is located in the Aitken basin – one of the largest, oldest and deepest basin on
 9 the Moon (Petro and Pieters, 2004). With reference to Fig. 6 the area is geologically diverse,
 10 containing rolling terrain with a moderately high density of craters less than 20 km in diameter
 11 (Nt), smooth light plains (Ip), and uplifted and complex faulted pre-basin bedrock covered by
 12 basin ejecta (NpNbr). Given the complexity of the terrain, is it possible that these features are
 13 simply uplifted bedrock surrounded by smooth plains?
 14

15 Although it is not possible to definitively determine the origin of these features from the
 16 imagery it can be shown that they are quantitatively different from the surrounding terrain.
 17 Sagan (1975) argued that deviations from thermodynamic equilibrium are a necessary (but not
 18 sufficient) condition of intelligent activity. He cited significant deviations from the blackbody
 19 radiation curve of Earth in the radio frequency portion of the electromagnetic spectrum as
 20 evidence of terrestrial intelligence, and went on to show that passive (electro-optical) imaging of
 21 Earth at resolutions (spatial scales) smaller than about 1 km reveals evidence of mechanical
 22 disequilibrium (e.g., rectilinear patterns of agriculture, road networks, etc.).
 23

24 Stein (1987) developed an algorithm that models images as fractals. Images of natural
 25 backgrounds, like the backgrounds themselves, exhibit a property known as self-similarity that
 26 have a distinctive power spectral density
 27

$$28 \quad S(f) \propto f^{5-2D} \quad (3)$$

29
 30 where $2 < D < 3$. Deviations from this curve, like that from blackbody radiation indicate possible
 31 non-natural, i.e., artificial phenomena. Stein’s algorithm has been used in several SETA
 32 investigations (Carlotto and Stein, 1990) and (Arkhipov, 1998).
 33

34 Analysis of the statistics of natural terrestrial backgrounds (forested areas, drainage patterns,
 35 tectonic features, etc.) and artificial features (e.g., roads, cities, vehicles, archaeological ruins)
 36 reveal artificial structures produce anisotropies in the 2D power spectrum at particular scales or
 37 resolutions (Carlotto 2007). A biologically-inspired target screener (Carlotto 2010) models the
 38 background using a bank of 64 Gabor filters, which measure the local power spectral density (4
 39 scales x 16 directions). The detection statistic
 40

$$41 \quad d = (\mathbf{x} - \mathbf{m})^T \mathbf{C}^{-1} (\mathbf{x} - \mathbf{m}) \quad (4)$$

42
 43 measures the deviation from the background, which is modeled as a Gaussian random variable
 44 with mean \mathbf{m} and covariance \mathbf{C} . The algorithm detects areas in the image containing objects with
 45 non-isotropic power spectra like buildings and vehicles (Fig. 7). Fig. 8 is the result of applying the

1 same algorithm to a portion of LRO frame M118769870L. The area is 4096x4096 pixels at 0.55
2 meters/pixel or about 507 sq. km. The local power spectra of the features under study as well as
3 several nearby craters appear to deviate significantly from that of the lunar background. These
4 objects are visually different from the background because their structure is different.

5 **5. Three-Dimensional Analysis**

6 Viewing the data in 3D further aids in our ability to understand the shape of these structures
7 and their relation to the background. Two images at different angles and similar sun angles can
8 be viewed side by side in stereo⁹. The Apollo 15 images AS15-P-8868 and AS15-P-8873 are good
9 candidates for stereo work as they were acquired from opposite but unknown viewing angles
10 (noted only as “fore” and “aft” in the metadata) at the same sun angle. Although feature A is
11 only about 10 pixels in size in the P frames and even smaller in the lower resolution M frames it
12 is apparent that the features are slightly lower in elevation than the terrain to the west (Fig. 9).

13
14 Available elevation maps of the moon do not have sufficient resolution to resolve the features
15 under study. Shape from shading (SFS), also called photoclinometry, is another method of
16 extracting height information from images (Horn 1977). SFS is useful in situations where the
17 reflectance characteristics and albedo are uniform across the scene and the image is acquired at
18 or near nadir. SFS methods assume an underlying scene reflectance function relating surface
19 gradients to image brightness. Pentland (1988) derives a linear approximation for the
20 Lambertian reflectance function, which is a good model for matte surfaces. A similar linear
21 approximation can be derived for the lunar surface. Embedding this within a strip integration
22 algorithm described by Horn (1977) we computed height maps from the two merged LRO
23 images, M118769870L and M1168450258L and averaged them together to create a relative
24 height surface.

25
26 At this point synthetic views can be generated in any viewing direction by an oblique parallel
27 projection of the merged image mapped onto the height surface (Foley and Van Dam 1983). Fig.
28 10a is a view at a 40° elevation angle looking northeast. From this viewing angle the southwest
29 end of feature A appears to be the “entrance” into the passageway. Fig. 10b is a reverse angle
30 view looking southwest that seems to show the passageway ending at the rise of terrain at the
31 other end.

32
33 Full pixel resolution northeast views of the two structures are shown in Fig. 11. There is
34 insufficient information in the imagery to determine the depth of the valley in between the two
35 walls. It is also not possible to determine if the valley ends or leads underground. The 3D view of
36 feature B reveals a radically different shape from that of A. What appears to be a long thin
37 depression is in fact a steep cliff. The top of B is concave with a rim along the opposite side. The
38 terrain surrounding the two structures is not flat but appears “excavated” by some unknown
39 mechanism.

40
41 Fig. 12 is a side by side overhead stereo view synthesized from the merged image and height
42 map demonstrating the relation of feature A with the background topography. It is evident that
43 the entrance end (indicated by the arrow) is lower in height than the other end (?), which may

43

⁹ <https://en.wikipedia.org/wiki/Stereoscopy>

1 or may not continue underground. Notice the depressed terrain immediately above and below
2 the feature. Could this area have been “excavated” by some mechanism, natural or artificial?

3
4 Fig. 13 is a perspective view of a wider area containing the features of interest generated from
5 M1153132512R¹⁰. Davies suggested the possibility of detecting abandoned alien mining or
6 construction operations on the moon (2012). As a point of comparison, the terrain surrounding
7 the features under investigation is not unlike that of the Bingham Canyon copper mine
8 southwest of Salt Lake City, Utah (Fig. 14). However the area immediately surrounding the
9 features lacks the terraced sides one would find in a terrestrial mine.

10 6. Discussion

11 Enormous quantities of lunar and planetary imagery are available to the public by way of the
12 Internet. While enabling a “citizen science” approach to SETI, the availability of so much data
13 also tends to generate new “discoveries” on a regular basis by those who want to discover
14 something such as alien bases, towers, construction and other activities on the lunar surface.
15 Although most of these findings turn out to be camera aberrations, image
16 compression/transmission errors, image enhancement artifacts, or simply misinterpretations of
17 unfamiliar surface features imaged in unfamiliar ways, some remain unexplained.

18
19 A decidedly conservative mainstream scientific establishment often rejects anomalies based on
20 subject matter alone, i.e., there cannot be alien artifacts on the moon because there are no
21 alien artifacts on the moon (or other planets). Such a view is an example of circular reasoning,
22 based on the belief that extraterrestrials do not exist, or if they do exist that they could not have
23 traveled to our solar system.

24
25 SETI has been criticized on epistemological grounds, i.e., we are looking for what we think is out
26 there (Denton 1984). In order to carry out an objective search for artificial features on the moon
27 and planetary surfaces, objective detection criteria must be established. Since we do not really
28 know what we are looking for, it is not possible to define in a direct way what is artificial. An
29 indirect approach is to develop a model of what is natural and detect deviations from the model
30 using anomaly detection. Several anomaly detection techniques that have been used in this way
31 include fractal models (Stein 1987), those discussed by Arkhipov (1998), comparative statistics
32 (Carlotto 2007), and the biologically-inspired method (Carlotto 2010) applied in Section 4. These
33 or other methods deployed in a cloud based or similar computing environment (e.g.,
34 seti@home¹¹) could be used by a global citizen science community to develop a list of candidate
35 sites for more in-depth investigation.

36
37 Based on the evidence presented in this paper we believe this area in Paracelsus C is one such
38 candidate that is worthy of future study by orbital missions and surface rovers. Both of the
39 features analyzed in this area are statistically different from the surrounding terrain. Feature A
40 has a structure unlike any feature seen on the moon to date. Its relation with the surrounding
41 terrain suggests an entrance and passageway that may lead underground based on 3D evidence,

41

¹⁰ http://wms.lroc.asu.edu/lroc/view_lroc/LRO-L-LROC-3-CDR-V1.0/M1153132512RC

¹¹ <http://setiathome.ssl.berkeley.edu>

1 with signs of excavation on both sides of the feature. Feature B also appears unusual but was
2 analyzed to a lesser extent.

3

4 Beyond the initial results presented here areas for additional work include collecting additional
5 imagery over the area at other solar/viewing angles in order to assess the interior structure of
6 feature A, refining the 3D models of features A and B (Section 5) using photometric stereo (Horn
7 1979) or other methods, and extending the background modeling and analysis (Section 4) to a
8 much larger area on the moon.

9 **References**

10 Carl Sagan, "Direct contact among galactic civilizations by relativistic interstellar spaceflight,"
11 *Planetary and Space Science*, Vol. 11, pp 485-498, 1963.

12

13 G. V. Foster, "Non-human artifacts in the solar system," *Spaceflight*, Vol. 14, pp 447-453, Dec.
14 1972.

15

16 C. Sagan, "The recognition of extraterrestrial intelligence", *Proceedings of the Royal Society*, 189,
17 pp.143-153, 1975.

18

19 B. K. P. Horn, "Understanding image intensities," *Artificial Intelligence*, Vol. 8, pp 201-231, 1977.

20

21 B. K. P. Horn, "Hill shading and the reflectance map," *Image Understanding Workshop*, Palo Alto,
22 CA 1979.

23

24 G. R. A. Freitas, "If they are here, where are they? Observational and search considerations,"
25 *Icarus*, Vol. 55, pp 337-343, 1983.

26

27 J. D. Foley and A. Van Dam, *Fundamentals of Interactive Computer Graphics*, Addison-Wesley,
28 Reading, MA, 1983.

29

30 T. Denton, "Dancing in our lenses: Why there are not more technological civilizations,"
31 *Journal of the British Interplanetary Society*, Vol. 37, pp 522-525, 1984.

32

33 M. C. Stein, "Fractal image models and object detection," *Society of Photo-optical*
34 *Instrumentation Engineers*, Vol. 845, pp 293-300, 1987.

35

36 A. Pentland, "The transform method for shape-from-shading," *MIT Media Lab Vision Sciences*
37 *Tech. Report 106*, July 15, 1988.

38

39 Mark J. Carlotto and Michael C. Stein, "A method for searching for artificial objects on planetary
40 surfaces," *Journal of the British Interplanetary Society*, Vol. 43, pp 209-216, 1990.

41

42 A. V. Arhipov, Earth-moon system as a collector of alien artefacts, *Journal of the British*
43 *Interplanetary Society*, Vol. 51, pp 181-184, 1998.

44

1 Noah E. Petro and Carle M. Pieters, "Surviving the heavy bombardment: Ancient material at the
2 surface of South Pole – Aitken Basin," *Journal of Geophysical Research*, Vol. 109, 2004.
3
4 Mark J. Carlotto, "Detecting Patterns of a Technological Intelligence in Remotely-Sensed
5 Imagery," *Journal of the British Interplanetary Society*, Vol. 60, pp 28-39, 2007.
6
7 Mark Carlotto, , "BiTS - A Biologically-Inspired Target Screener for Detecting Manmade Objects
8 in Natural Clutter Backgrounds," *SPIE Defense and Security*, 5-9 April 2010, Orlando, Florida
9 (Paper 7697-37).
10
11 P.C.W. Davies, "Footprints of alien technology," *Acta Astronautica*, Vol. 73, pp 250–257, 2012.
12
13 P. C. W Davies and R. V. Wagner, "Searching for alien artifacts on the moon," *Acta Astronautica*,
14 Vol. 89, pp 261-265., 2013
15
16

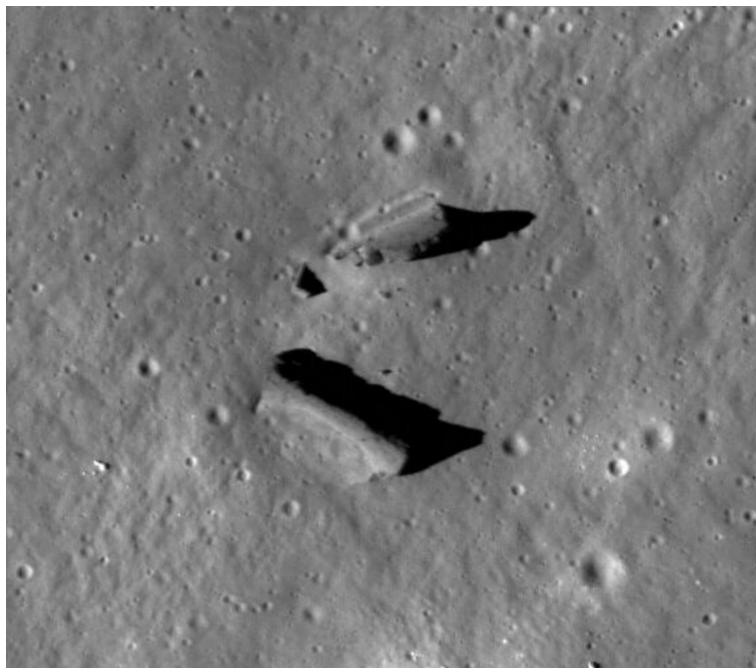
1

Table 1 Apollo and LRO images over the area of interest

Frame	Resolution (meters)	Solar Elevation ¹²	Emission Angle ¹³	Incidence Angle ¹⁴	Phase Angle ¹⁵
AS15-P-8868		14	(forward) ¹⁶		
AS15-P-8873		14	(aft) ¹⁷		
AS15-M-0081	6.4	14			
AS15-M-0082	6.3	14			
AS15-M-0083	6.3	15			
AS15-M-0084	6.5	16			
AS15-M-0085	6.5	16			
M118769870L	0.55		1.7	68.9	70.5
M1115441699L	0.8		1.7	34.4	35.8
M1153132512R	0.94		1.2	58.7	57.6
M1168450258L	0.90		1.7	54.6	56.3

2

3



4

5 **Fig. 1 High resolution (0.55 meters/pixel) image of unusual structures discovered by Ridge in**
 6 **LRO frame M118759870L (north is down).**

6

¹² Angle between ray directed toward the sun and the surface of the moon.

¹³ Look angle of ray directed toward the sensor and the local surface normal (nadir).

¹⁴ 90° – solar elevation angle.

¹⁵ Angle between the emission and incidence angle.

¹⁶ Value not provided in image metadata record

¹⁷ Ditto



LRO/LROC-NAC Observations at point (testing Map Projected NACs)

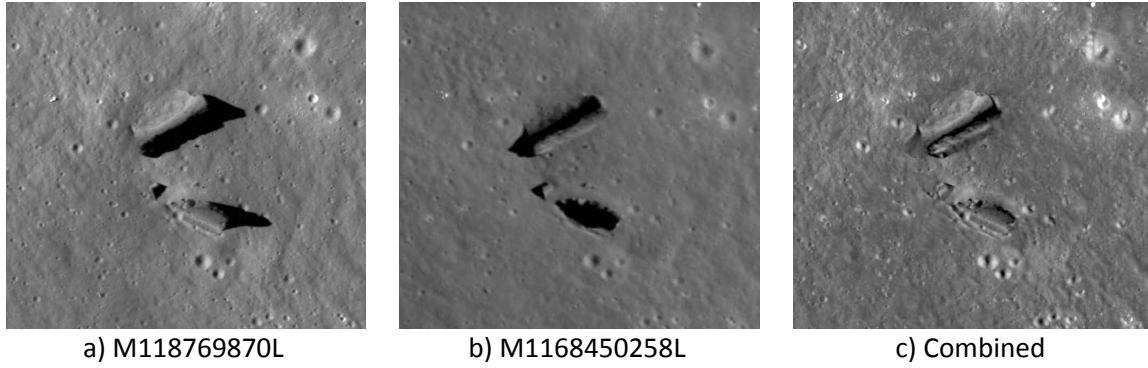
To request another location, enter lat,lon in decimal and press submit.

lat: lon:

Preview at (lat, lon) = (-21.6479, 165.212)				Image
100 mpp 15000 meters	25 mpp 3750 meters	5 mpp 750 meters	1 mpp 150 meters	
				M118769870L
				M1115441699L
				M1153132512R
				M1168450258L

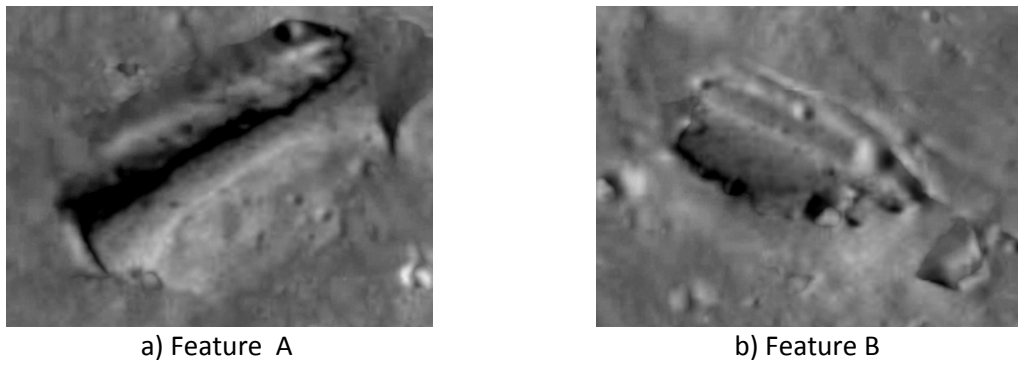
- 1
- 2
- 3
- 4
- 5

Fig. 2 LRO image search using Planetary Imagery Processing Environment (PIPE)



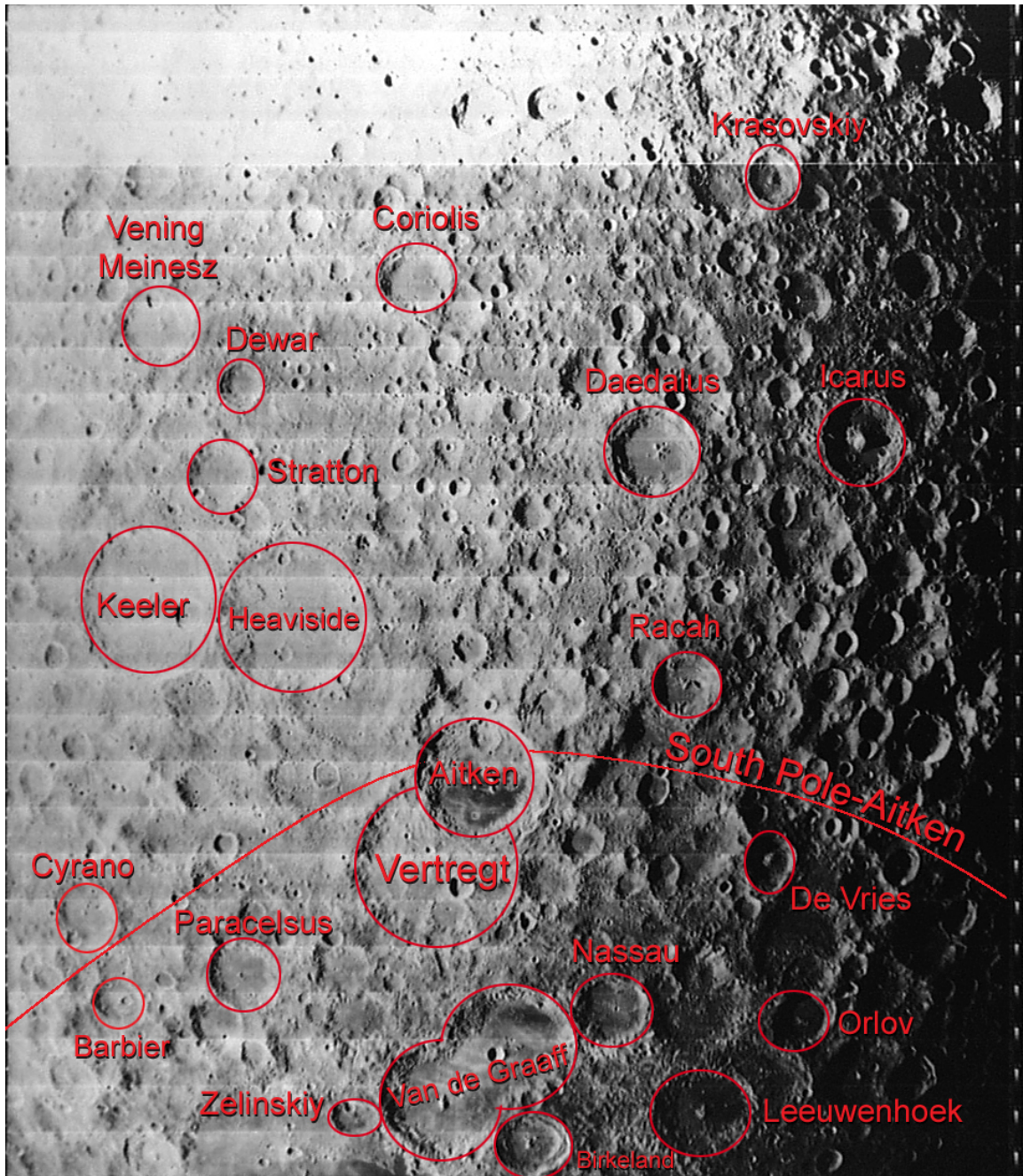
1
2
3

Fig. 3 Merging registered images using shadow pixel replacement (north is up)



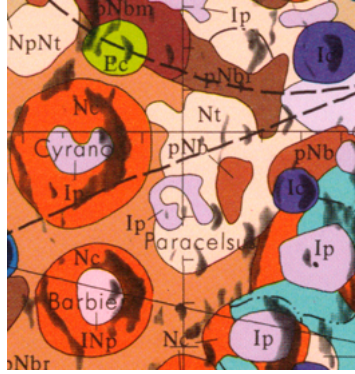
4
5
6

Fig. 4 Close up (full pixel resolution) merged images. Images have been rotated to the viewing direction (north is down).



1
2
3
4

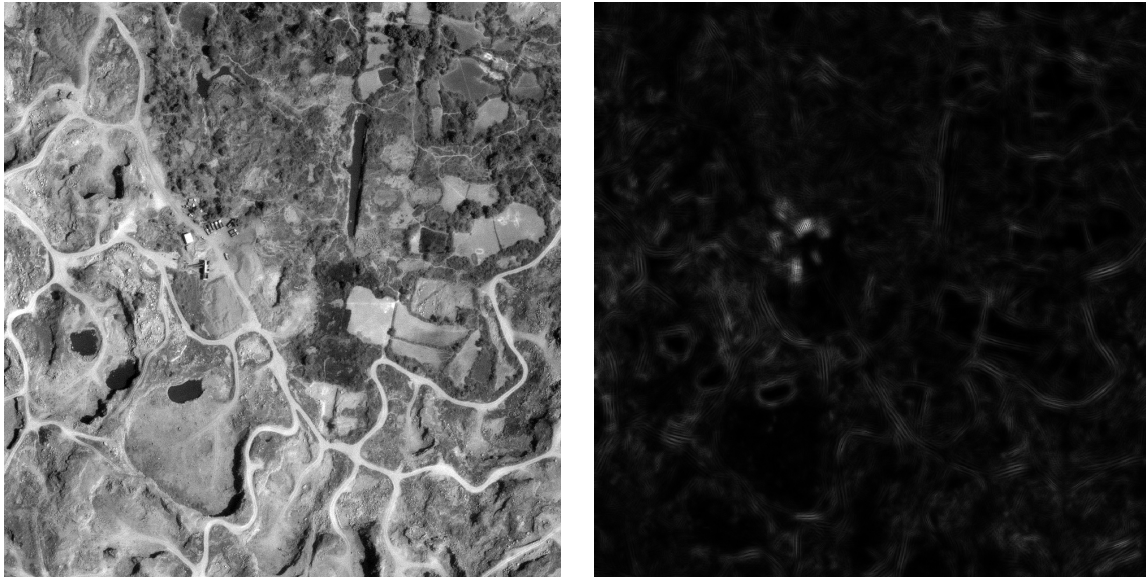
Fig. 5 Paracelsus C is a satellite crater of Paracelsus located in the Aitken basin on the far side of the Moon.



1

2 **Fig. 6 Section of Geologic Map of the Central Far Side of the Moon¹⁸ over the crater**
3 **Paracelsus.**

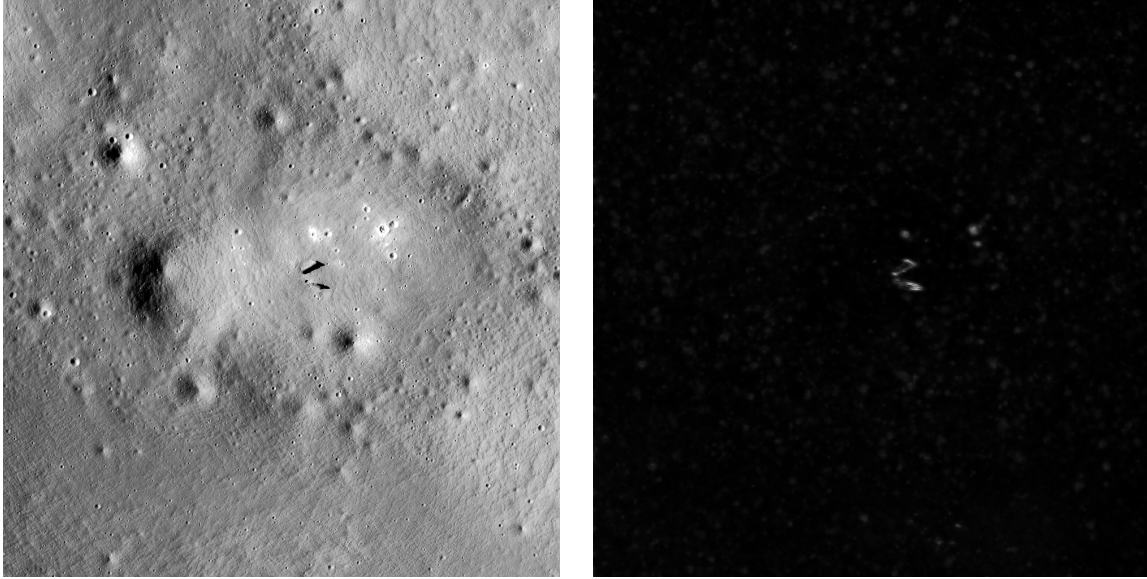
4



5 **Fig. 7 Small buildings and vehicles in GeoEye image (left). Image of deviations from**
6 **background model (right).**

7

7
¹⁸ <http://www.lpi.usra.edu/resources/mapcatalog/usgs/>



1 Fig. 8 Portion of vertically-flipped LRO image M118769870L centered over structures (left).
2 North is up. Image of deviations from background model (right).

3



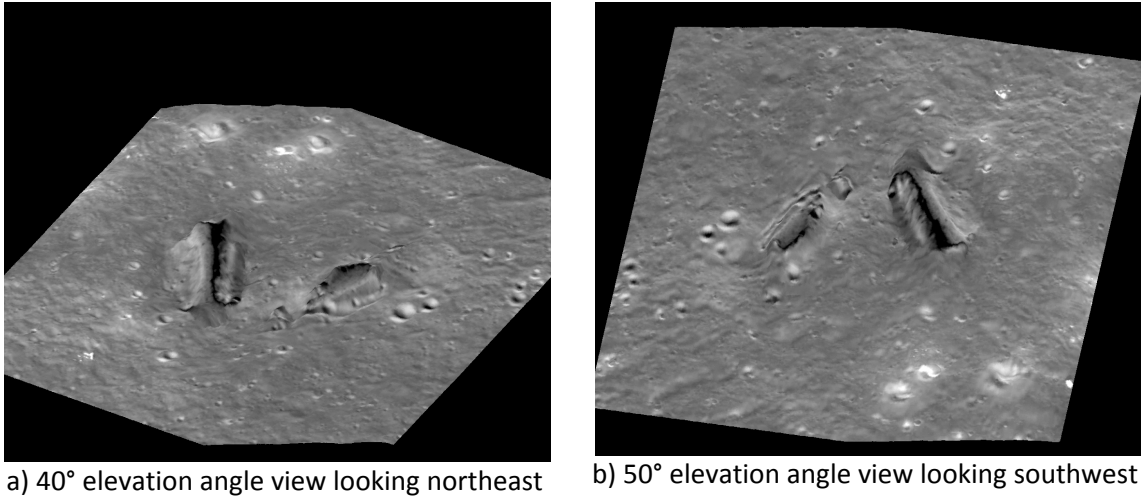
4

5

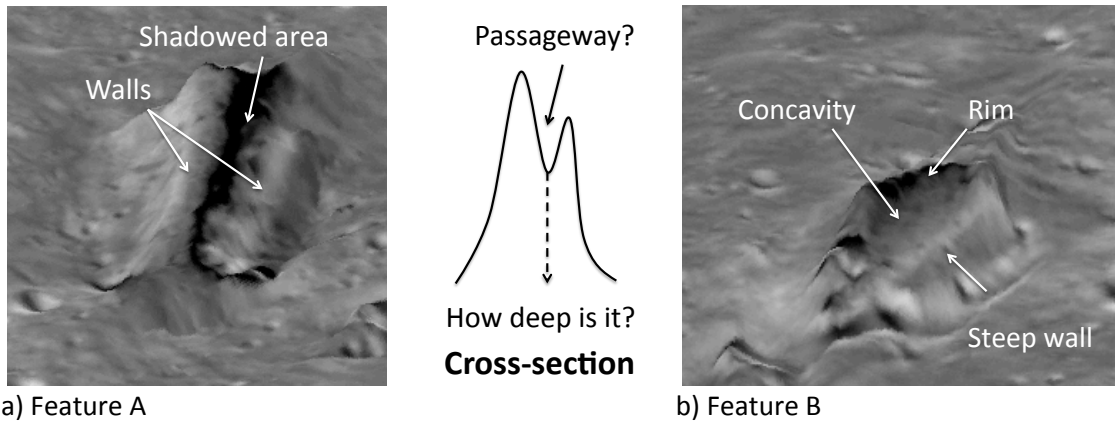
6

7

Fig. 9 Stereo pair constructed from AS15-P-8868 and AS15-P-8873. North is left. View is looking east. Notice the sun angle is similar to that in M118769870L.



1 **Fig. 10 Two synthesized oblique views computed from the merged image and SFS-derived**
2 **height map**



3 **Fig. 11 Details of 3D renderings in 40° elevation angle northeast view**

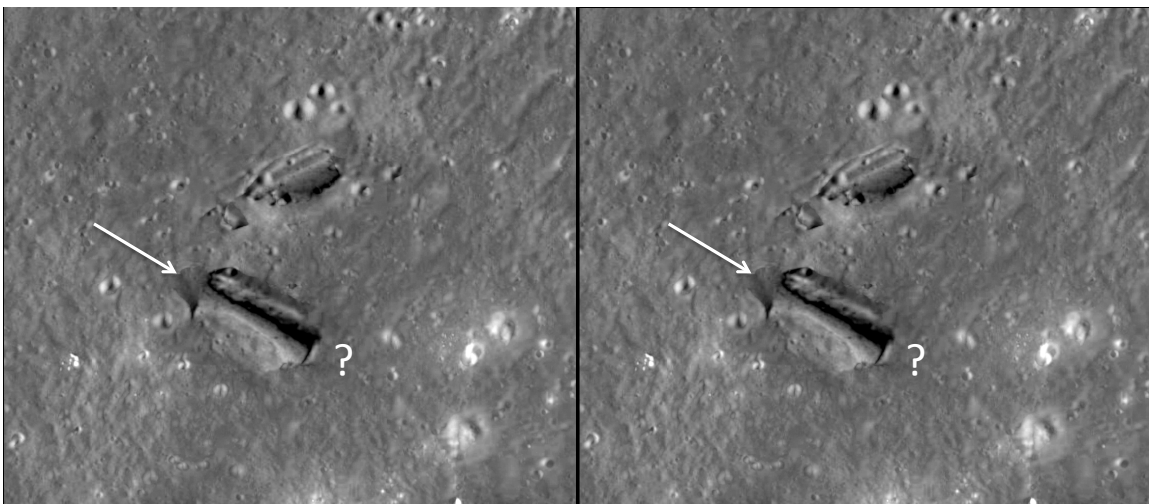
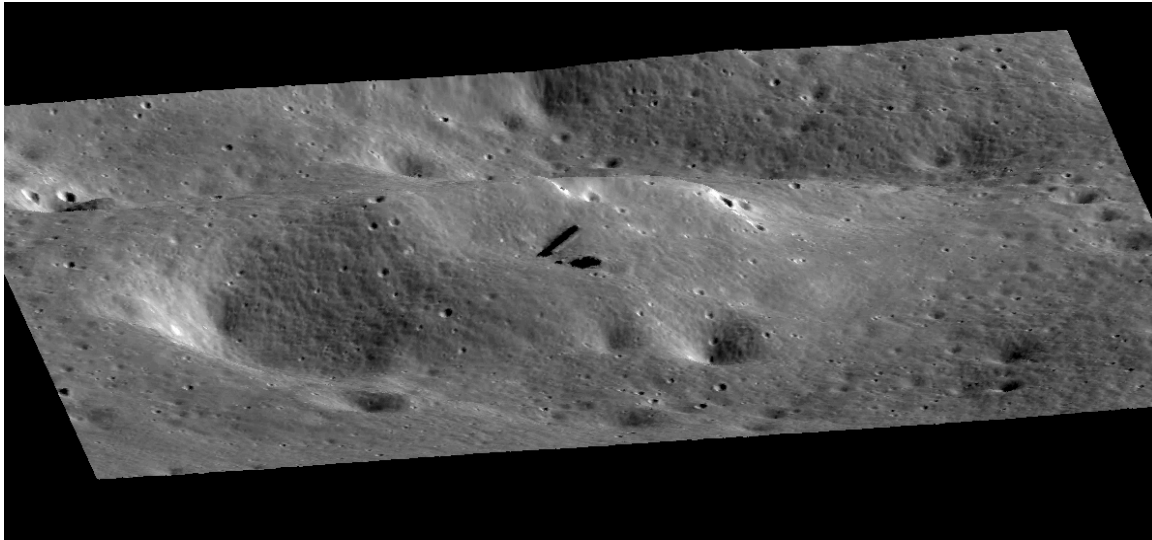


Fig. 12 Synthesized overhead stereo view. Arrow indicates entrance end of feature A. Whether other end (?) continues underground is unknown.

1



2

3 **Fig. 13** Perspective view of surrounding area generated from M1153132512R. Features A and
4 B are in the middle. The sun angle is opposite that of M118769870L.



5

6 **Fig. 14** Bingham Canyon Mine, Utah, USA (Image courtesy Michael Lynch)¹⁹

6

¹⁹ <http://whenearth.net/awe-inspiring-aerial-images-worlds-mega-mines/>